Primary ^{29}Si hyperfine structure of E' centers in nm-sized silica: Probing the microscopic network structure

A. Stesmans, K. Clémer, and V. V. Afanas'ev
Semiconductor Physics Laboratory, Department of Physics, and INPAC-Institute for Nanoscale Physics and Chemistry, University of Leuven, Belgium

(Received 14 March 2007; revised manuscript received 28 December 2007; published 25 March 2008)

Point defects in fumed ~7-nm-sized fumed silica nanoparticles have been studied by *X*-, *K*-, and *Q*-band electron spin resonance (ESR) following 10-eV irradiation. The E' defects are monitored as a function of post manufacture heat treatment with the sample brought into contact with "bulk" Si/SiO_2 entities at elevated temperatures in vacuum ($T_{an}=1005-1205$ °C), i.e., the presence of an Si/SiO_2 interface. This results in a drastic increase in E' defect density with increasing T_{an}, enabling us to resolve the primary ^{29}Si hyperfine (hf) structure of the E' centers located in the core region of the nanoparticles. Detailed analysis of the observed hf spectra reveals several items pointing to a modification of the specific network structure of the core region of the nanoparticles. An increased hf splitting of 438 ± 2 G is observed compared to bulk silica (418 ± 2 G) indicating that the core part E' centers exhibit a more pyramidal defect structure. Moreover, the increased primary hf splitting indicates that the core of the fumed silica particles is densified, possibly associated with the presence of more low-membered rings in the nm-sized silica network.

DOI: 10.1103/PhysRevB.77.094130 PACS number(s): 61.46.Df, 61.72.J−, 68.35.Dv, 76.30.Mi

I. INTRODUCTION

It is well established experimentally that the electrical and optical properties associated with the fumed silica nanoparticles distinctly differ from those of their bulk silica counterparts.[1–3] Better understanding of these properties may be obtained from detailed information about the exact structure of these nanoparticles. Driven by this goal, fumed silica has been intensively studied theoretically as well as by a range of sensitive experimental techniques such as positron annihilation[4] and x-ray diffraction,[1] and the key photon-solid interaction probes including optical[2] and Fourier transform infrared (FTIR) absorption,[1,3,5] Raman spectroscopy,[1] nuclear magnetic resonance (NMR),[6] and electron spin resonance (ESR).[2,7–9]

In addition to the fact that the nanoparticles are in the amorphous phase, interpreted as being caused by the extremely fast cooling of the pyrogene silica aggregates formed at 1400–1800 °C, very little is known about their exact structure. Based on results of infrared and Raman studies, Uchino *et al.* suggested a more flexible network structure for the silica nanoparticles as compared to bulk SiO_2 consisting of enhanced densities of 3 and 4 membered rings.[1] Though being the tool eponymous for point defects with atomic level physicochemical sensitivity,[10–12] little research has so far been carried out using ESR: Up to recent ESR work[8] the few attempts to discern ESR signals originating from the nanoparticles failed,[4,7] possibly due to magnetic inactivity of the occurring defect centers. Combining ESR analysis with post formation heat treatment and (~10 eV) photon excitation resulted in the observation of various ESR active point defects, including the familiar E'_γ center, *EX*, the peroxy radical (POR), the methyl radical, and an axially symmetric center of unknown origin. In these observations, the E'_γ data had drawn particular interest because of the potential to provide information on the structure and uniformity of the network throughout the particles. This work proceeds along these lines, where through observation of the ESR hyperfine (hf) structure of E'-type centers, it is aimed to asses nanoscopic details of the silica nanoparticles structure.

A. E'_γ centers in fumed silica

Studying the ESR characteristics of the observed E' signals provided useful information about the defect's local environment.[8] Plausible evidence was inferred for the presence of two distinct systems of E' centers. The two systems were interpreted as one pertaining to the core, the other to the surface region of the nanoparticles. The ESR features of the E' centers in the core region were very similar to those of the common E'_γ center[13,14] (generic entity $O_3\equiv Si^{\cdot}$) present in bulk a-SiO_2. The outer region E' centers, however, exhibit different properties such as a shift in zero crossing g value (g_c) towards higher values ($\Delta g_c\sim0.0002$). Such g value alterations are the reflection, through the spin-orbit coupling, of structural variations affecting the spatial distribution of the unpaired electron orbital. Modification of the defect structure towards a more planar or pyramidal defect configuration would directly translate into a shift in g value. However, to get a conclusive explanation for the g shift observed for the surface E' center in the fumed silica nanoparticles in terms of structural modification will require correct theoretical insight, which appears at present unavailable. In another approach, one could try to "translate" observed g shifts into specific structural modification via inference of the latter through an independent experimental way.

From the observed E' features it was concluded that the core region and the outer region of the nanoparticles exhibit a dissimilar network structure: While the core region is very bulk a-SiO_2-like, the surface and near surface layers seem to suffer from enhanced amorphous state disorder and strain. Moreover, the surface E' system appeared to be more apt to environmental chemical and physical interaction (adsorption) impact as the centers became largely ESR inactive when

leaving the nanoparticles for some time in room ambient after VUV activation. The number of E' surface centers was also found to be reduced by post-manufacture heating at elevated temperatures ($T_{an} \geqslant 800$ °C). One possible mechanism here is the attendant decrease in the specific surface area due to sintering.[1] The maximum E' density encountered in fumed silica was found to be small as compared to standard thermal a-SiO_2 grown[15] on Si, indicating that the nanoparticles are oxygen rich, i.e., low density of O vacancies.

B. Primary ^{29}Si hyperfine splitting of the E'_γ center

As a consequence of the low E'_γ density encountered, even after exhaustive VUV irradiation, we were, at that point,[8] unable to discern any hf splitting originating from the observed E' centers involving the weakly abundant ^{29}Si (4.7 at. %) nuclei. The primary ^{29}Si hf structure of the E'_γ center in γ-irradiated a-SiO_2 was observed first by Griscom *et al.*[16] revealing a primary doublet splitting of ~420 G. From these results detailed information about the short-range structure of the amorphous network, such as, e.g., distribution of O-Si-defect bond angle θ (angle between the unpaired orbital and a Si-O backbond) and bond angle, could be extracted. Other interesting work illustrating the power of E' primary hf structure in providing pertinent information was reported by Devine and Arndt.[17,18] Comparison[17] of the primary hf structure of the E' centers observed in ^{60}Co γ-irradiated undensified and densified suprasil did provide, not depending on the type of silica (suprasil) used, some fundamental insight as to the microstructural changes induced by densification. Densification of the silica of 24% was observed to result in an increase of the isotropic hf splitting to ~465 G, from where was inferred an increase in the length of the Si-O back bonds (by ~0.36%) of the defect tetrahedron, a reduction (by ~5.1°) of the mean bridging Si-O-Si bond angle of the defect back bonds, and puckering of the average E' center so that θ increases by ~1° (associated with an equivalent decrease of the tetrahedral O-Si-O bond angle). Though not qualitatively, the quantitative aspect of the inferences made may be less convincing (*vide infra*).

Along these lines, it appears that the observation and analysis of the primary ^{29}Si hf structure of the E' center in the fumed silica nanoparticles and bulk silica could possibly provide us with independent detailed information on atomic scale structural changes induced by the "nanosize" aspect of the fumed silica particles—a major target of this work. However, for sensitivity reasons the number of E' centers in the ESR sample should increase drastically to enable one to resolve the hf splitting associated with the small abundant ^{29}Si nuclei (nuclear spin $I=\frac{1}{2}$; 4.69 at. %). In our previous work[8] the nanoparticles were subjected to post manufacture heating in vacuum in the temperature range $T_{an} \sim 850-1115$ °C combined with exhaustive VUV activation of the E' centers. Upon prolonged VUV activation, a maximum E' density of $\sim 2.4 \times 10^{15}$ g^{-1} could be attained for the as-grown particles, a density still at least one order of magnitude too small to enable ^{29}Si hf detection. Thus, any success here would require a drastic increase in density of embedded E' centers.

C. Interactions with SiO at elevated temperatures

It has been observed for thermal oxide on Si and for fused silica that the interaction of the SiO_2 network with SiO at elevated temperatures results in a significant increase in E' density. In previous work on the structure of thermal oxide on Si,[19] the influence of post-deposition heat treatment in an O_2-deficient ambient in the temperature range T_{an} = 950–1250 °C was studied. The main motive for this work was probing by ESR via generated point defects of the electrically and morphologically well known thermal degradation process effectuated by such annealings to the thermal Si oxide on Si (see, e.g., Refs. 20 and 21). In another ESR work the interaction of fused silica with gaseous SiO, *in situ* provided from coinserted solid SiO, during annealing at ~1140 °C was studied.[22] One of the incentives for these studies was the suspicion raised about the influence of Si/SiO_2 interface-released SiO molecules: Indeed previous work had observed the formation of pores (voids) through the SiO_2 film evidencing the freeing of volatile SiO at the Si/SiO_2 interface through the net reduction reaction $Si(s) + SiO_2(s) \rightarrow 2SiO$ (volatile).[20] Later, the process of outdiffusion and subsequent desorption of the volatile SiO from thermal Si/SiO_2 was evidenced more directly by x-ray photoelectron spectroscopy during post oxidation vacuum annealing at 800 °C.[23] The question remained whether the outdiffusion of gaseous SiO would modify the SiO_2 network. It was found that the SiO did indeed affect on the SiO_2 network, in fact aggressively degrading it. Such information was revealed through the observation of several types of generated defects including E'_γ, E'_δ, EX, and the predominant exclusive S center. A specific finding was that the interaction of the SiO_2 network with SiO at elevated temperatures resulted in an increase in E'_γ density. If, in the interest of the current study, the fumed silica network could be influenced by the SiO in a similar way when it comes to E' defect generation, this approach might allow us ultimately to detect the primary ^{29}Si hf structure of the E' centers in the nanoparticles.

Stepping from these results, we have in this work exploited the detrimental potential of SiO to the benefit, i.e., enhancing the E'_γ density in the fumed silica network, which has enabled detection of the primary ^{29}Si hf structure. In this approach we will demonstrate that through its analysis one can obtain atomic-scale structural information. The hf parameters of the E' centers observed in fumed silica are compared to those observed in bulk silica independently revealing differences in the network structure.

II. EXPERIMENTAL DETAILS

A. Samples

The samples studied were taken from high-purity pyrogene fumed silica powder of 7 nm average particle size and 380 ± 40 m^2/g surface area, with a "bulk" density of 36.8 g/dm^3 and low metallic impurity content.[24] The material is in the amorphous state. As specified, the particles are fabricated by burning silicon tetrachloride in an oxygen-hydrogen flame at ~1800 °C. During particle formation and subsequent cooling down, interparticle collisions and subsequent fusion results in the formation of chainlike aggregates from 10 to 30 units (fume particles) or, put differently, from ~0.1 to 0.2 μm in length. Separate samples (fresh ones for

each thermal step) were subjected to postmanufacturing baking in vacuum (base pressure $\leqslant 4\times10^{-6}$ Torr) for ~3 h at desired temperatures (T_{an}) in the range 1005–1205 °C. Each heating procedure was carried out with a suitable amount of the powder tightly sandwiched between two (fresh) slices of Si wafer (0.47 nm thick) with a standard thermal SiO_2 (6.5 nm) on top, the SiO_2 film facing the inside of the sandwich.

After an initial ESR test, to maximally reveal defects, the samples (both in the as-grown state and after additional heat treatment) were subjected at room temperature (RT) to prolonged irradiation by VUV (~10 eV) photons (flux $\sim10^{15}$ cm^{-2} s^{-1}) to photodissociate H from passivated defects. Possibly, the treatment may additionally unveil strained or weak bondings (bond rupture).[18,19,21] This, however, would also add to the ultimate goal, that is, acquiring atomic scale information about the SiO_2 particles network, as these sites of defect creation, i.e., strained and/or weak bonding sites, constitute in embryo also imperfections in the a-SiO_2 matrix, although not necessarily concerning nonstoichiometry. Further discussion can be found in Ref. 8. For reference, measurements were also carried out on a suprasil I synthetic silica[25] sample subjected to 100 Mrad ^{60}Co γ irradiation at 300 K.

B. Electron spin resonance spectroscopy

Conventional CW absorption-derivative ESR measurements were performed at X (~9.2 GHz; Jeol JES-FA100 spectrometer), K (~20.4 GHz), and Q band (~33 GHz) in the temperature range 77–110 K. The levels of the magnetic field (**B**) modulation B_m and incident microwave power P_μ were properly watched to avoid signal distortion. More details can be found in Ref. 11. The hf signals were measured in an (out-of-phase) second harmonic detection mode in the Q band at relatively high modulation amplitudes (2 G) and microwave powers (5 mW).[26,27] Typically, an ESR sample comprised ~2–3 mg of fumed powder. After VUV irradiation, defects were found to undergo modification when left in room ambient over time. Hence, to study the characteristics of modification, ESR measurements were performed immediately upon VUV irradiation as well as after leaving the samples in room ambient for desired times (~3 days). For g factor and defect (spin) density determination, use was made of the P donor resonance of a calibrated Si:P marker sample [spin $S=1/2$; $g(100\ \mathrm{K})=1.99891$] comounted with the studied samples and recorded in the same trace.

III. RESULTS

A. SiO impact

As reported before, no ESR signal could be observed in the as-fabricated silica particles. After the vacuum anneal in the presence of SiO release (henceforth referred to as SiO-vac. anneal) at various temperatures followed by VUV irradiation the situation changes drastically. Several defect centers are observed including *EX*, the POR, the nonbridging oxygen hole center (NBOHC), and E'-type centers. In this work we will focus on the latter defects. Figure 1 shows

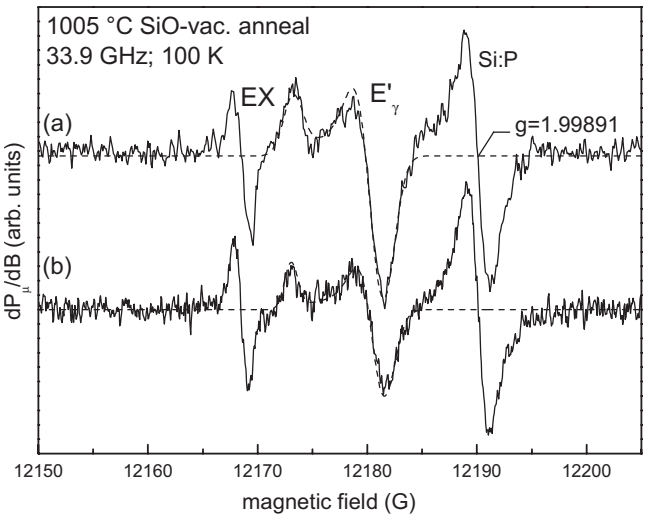

FIG. 1. Q-band ESR spectra of the fumed silica nanoparticles subjected to SiO-vac. annealing at 1005 °C measured at 100 K (a) immediate upon additional VUV irradiation and (b) several days later, the sample being left in room ambient. The dashed curves represent spectra simulations employing Gaussian broadening functions. The g values used for both simulations are (a) $g_1=2.00168$, $g_2=2.00058$, $g_3=2.0003$; (b) $g_1=2.00171$, $g_2=2.00053$, $g_3=2.0003$. The signal at $g=1.99891$ stems from a comounted Si:P marker.

representative Q-band spectra recorded on a $T_{an}\sim1005$ °C sample (a) immediately upon VUV activation and (b) several days later, the sample being left in room ambient. The characteristic central-line two-peak powder pattern signal observed is seen to be much similar (e.g., regarding width, overall shape, and g matrix) to that of the common E'_γ variant[13,14] in bulk silica, characterized by the principal g matrix values $g_1=2.0018$, $g_2=2.0006$, and $g_3=2.0003$.

The E' spectra recorded immediately after VUV irradiation and those measured after leaving the samples for a substantial time in room ambient could be well simulated (see Fig. 1; dashed curves) using similar ESR parameters (g values and constituent line widths). For the various T_{an} values an average drop in E' density by a factor $\sim1.6\pm0.5$ is observed after leaving the sample for substantial time (~days) in room ambient. The experimental observed decay rate shows a slight tendency to decrease with increasing T_{an}, the variations, however, being well within the experimental error. As reported previously,[8] a similar reduction has been observed for fumed silica subjected to simple vacuum annealing (i.e., no copresent SiO release) at various T_{an}. A main finding here is that compared to ordinary vacuum annealing, the SiO-vac. anneal results in a drastic enhancement of E' density increasing with T_{an} to a maximum defect density of $(4\pm1)\times10^{17}$ cm^{-3} (~1.7 ± 0.4 g^{-1}, using a specific gravity of 2.3 g cm^{-3}) attained for $T_{an}=1205$ °C, as illustrated by Fig. 2. For the sample SiO-vac. annealed at $T_{an}\sim1105$ °C the attained E' density is over a 100 times larger than for the standard annealed sample.

Another notable observation appears from Fig. 3 showing zoomed in representative ESR spectra of samples subjected to SiO-vac. annealing [Fig. 3(a)] and vacuum anneal-

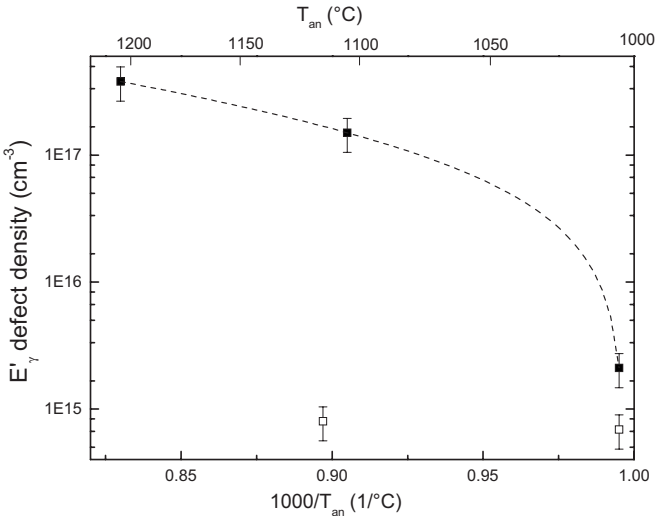

FIG. 2. Defect densities of the E'_γ defect inferred from K-and Q-band ESR in fumed silica subjected to a ~3 h SiO-vac. anneal (solid symbols) or a ~1 h standard vacuum anneal (open symbols) at various temperatures subjected to ~1 h VUV irradiation. The measurements were performed immediately after the VUV activation. The dashed curve is merely meant to guide the eye.

ing [Fig. 3(b)] at $T_{an} \sim 1005$ °C recorded immediate upon VUV irradiation. The latter spectrum was obtained from a previous study (see Ref. 8). From this comparison it can be seen that the E' g_c of the nanoparticles subjected to the SiO-vac. anneal has not noticeably shifted with respect to the general bulk value ($g_c \sim 2.00055$). By contrast, g_c for the sample subjected to the vacuum anneal has shifted upward to ~2.00065.

B. Hyperfine structure

As alluded to, the realized increase in E' density has enabled us to observe the ^{29}Si hf structure related to E' defects.

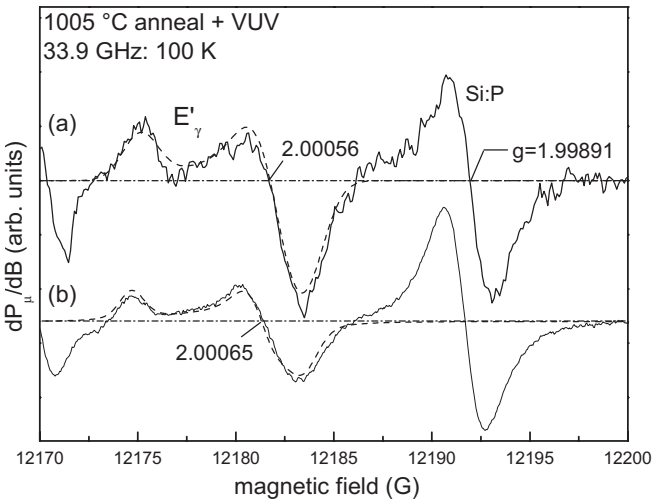

FIG. 3. Powder pattern Q-band ESR spectra of the E' signal measured upon VUV activation on fumed silica nanoparticles subjected to (a) a SiO-vac. anneal at 1005 °C and (b) a standard vacuum anneal at 1005 °C. The dashed curves represent spectra simulations. The lower S/N ratio for spectrum (a) compared to (b) is due to the smaller amount of sample available.

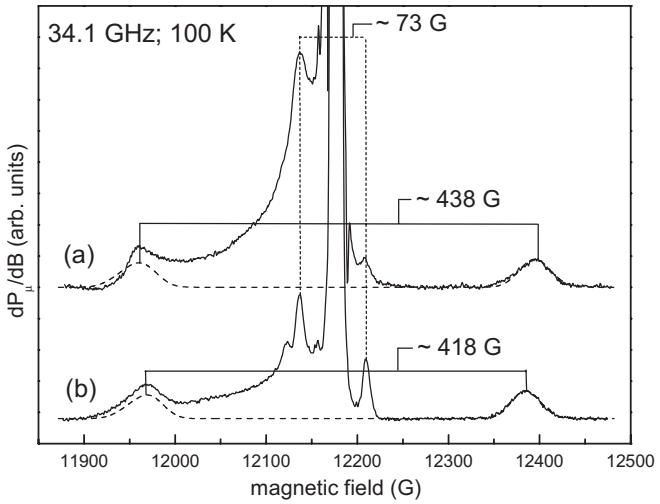

FIG. 4. High power (saturation) second harmonic Q-band spectra for (a) fumed silica subjected to a ~1105 °C SiO-vac. anneal and additional VUV irradiation measured at 100 K after leaving the samples for substantial time in room ambient and (b) Suprasil I synthetic silica subjected to 100 Mrad ^{60}Co γ irradiation. The dashed curves represent simulations of the primary ^{29}Si hf structure of the E' centers, obtained using the principal g matrix values $g_1 = 2.0017$, $g_2 = 2.0005$, $g_3 = 2.0002$ and hf parameters (a) $A_{iso} = 436$ G, $A_{aniso} = 22$ G and (b) $A_{iso} = 418$ G, $A_{aniso} = 22$ G. Spectra were aligned at the resonance field of the E' central resonance.

Figure 4(a) shows a typical high-power second harmonic mode Q-band spectrum observed for the fumed silica nanoparticles subjected to SiO-vac. annealing at 1105 °C and additional VUV irradiation after leaving the sample for days in room ambient. For reference we also performed a similar measurement [Fig. 4(b)] on suprasil I synthetic silica subjected to 1 MGy ^{60}Co γ irradiation at 300 K. In both samples two doublet structures are observed. The central line, largely off scale, corresponds to the E'_γ centers with no hf splitting (unpaired electron located on ^{28}Si or ^{30}Si nuclei of $I=0$). The broad absorption line overlapping with the low-field parts of the doublets originates from oxygen hole centers (OHC's).

The inner hf doublet—henceforth referred to as the 73-G doublet—exhibits a splitting of 69 ± 4 G and 73 ± 2 G for the nanoparticles and suprasil, respectively. More zoomed-in spectra, better displaying the inner doublet in fumed silica and suprasil are shown in Fig. 5. A similar doublet has been observed previously in various types of a-SiO_2 and was attributed[27,28] to O_2=Si·-H (the black dot symbolizes the E' unpaired electron) entities with an H atom in a back bond instead of O. It should be noted that this doublet, relative to the E'_γ signals, appears less prominent in the fumed silica powder than in the suprasil sample.

The outer doublet (referred to as 418-G doublet) is, within the lines of this work, of more interest as it concerns the well-known primary ^{29}Si hf splitting of the E' center.[16,29] The measured hf splittings are 438 ± 2 G and 418 ± 2 G for the nanoparticles and suprasil, respectively (see Fig. 4), bearing out a noticable increase in hf spitting for fumed silica.

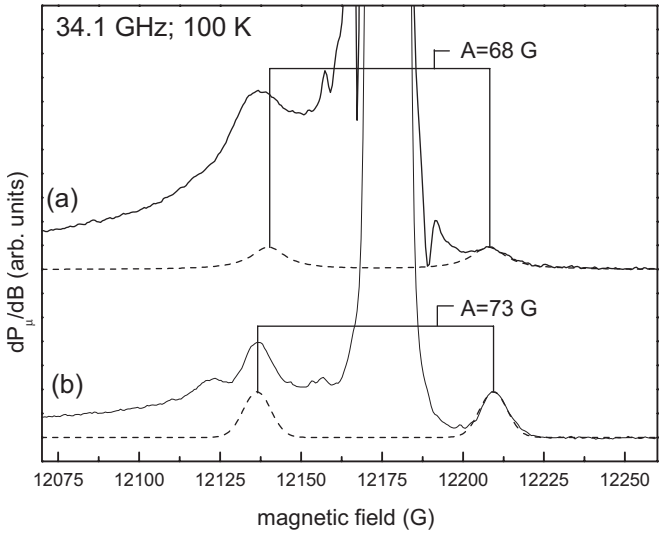

FIG. 5. Zoomed-in high power (saturation) second harmonic Q-band spectra for (a) fumed silica subjected to a ~1105 °C SiO-vac. anneal and additional VUV irradiation measured at 100 K after leaving the samples for substantial time in room ambient and (b) Suprasil I synthetic silica subjected to 1 MGy ^{60}Co γ irradiation. The dashed curves represent simulations of the H hf structure of the H associated E' centers (O_2=Si˙-H), obtained using the isotropic g value g=2.0019 and hf parameter (a) A=69 G and (b) A=73 G. Spectra were aligned at the resonance field of the E' central resonance, and scaled to equal E' intensity.

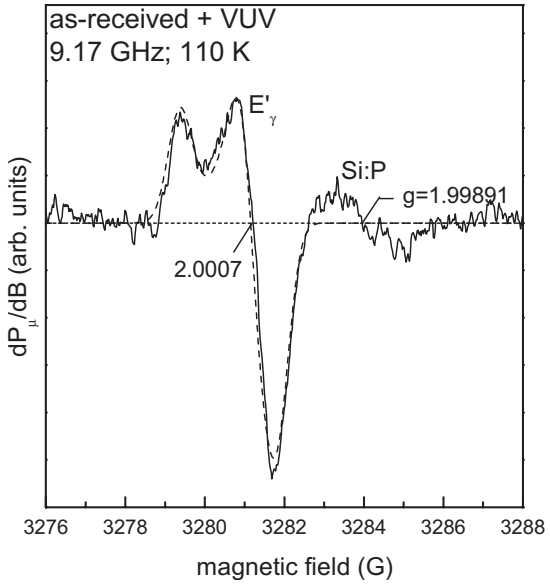

FIG. 6. Powder pattern derivative-absorption X-band ESR spectrum of the E' signal measured immediate upon VUV activation of the as-received fumed silica nanoparticles, using P_μ=0.1 mW, B_m =0.6 G, and averaging over ~50 scans.

C. Surface E' system

As reported before,[8] the E' centers ascribed to defects located in the surface layers of the nanoparticles exhibit a slightly larger g_c than E'_γ centers in bulk silica. In a first interpretation, this was ascribed to a change in the defect's morphology (configuration) (e.g., variation in pyramidal angle), which may seem plausible for a defect system that would pertain to surface layers. Recently, however, it came to our attention that a similar increase in g_c has been reported before for E'-type defects with an OH group in the back bond (O_2=Si˙-OH) located at the surface of high purity quartz[30,31] which would point to a rather chemical origin for the variations in g. In search for the true atomic nature of the surface E' system (previously estimated at ⩾70% of all E' defects observed in the as received state), we therefore, as an additional test, subjected the as-received silica nanoparticles immediately upon VUV irradiation to intensive X-band ESR measurements trying to resolve possible (weakly splitted) H hf structure resulting from the back bonded OH entity. A representative spectrum is shown in Fig. 6.

IV. ANALYSIS AND DISCUSSION

A. Surface E' centers

In a previous work we compared the principal g values of several generic E' centers in irradiated high purity silica and synthetic quartz silica. Remarkably, it was noticed that, in contrast to the findings in fumed silica, the surface E' (E'_s) centers observed in crushed silica particles and thin deposited a-SiO_2 films on Si are characterized by a slightly smaller g_c.[32,33] However, there is one E'-type surface center, not included in the previous comparison, that does exhibit an increased g_c value. Radzig reported[30,31] an E'-type defect center with principal g values g_1=2.0003, g_2=2.0007, and g_3=2.0019, values very similar to those we reported for the E' centers located in surface layers of fumed silica. Radzig attributed the defect to a O_2=Si˙-OH entity with an OH group in a back bond, located at the surface of high purity quartz. Identification of the defect was accomplished through the observation of the primary ^{29}Si hf splitting (A_{iso}=413 G; A_{aniso}=19 G) and the small ^{1}H hf splitting (A_{iso}=2.2 G; A_{aniso}=0.6 G).[30]

The presence of such a defect site at the surface of the fumed silica nanoparticles may not be totally unexpected as extensive NMR studies[6] have pointed out that large concentrations of silanols (Si-OH groups) are present at the surface of fumed silica. If the observed surface E'-type defects in the nanoparticles would have such a OH group in the back bond, the central line should show additional structure resulting from the hf interaction with the ~100% abundant ^{1}H nucleus. No such features could be observed in the previously reported K- and Q-band spectra recorded immediate upon VUV activation of the as-received samples. However, it is possible that when measuring at these (high) frequencies the hf splitting remains unresolved as a result of intrinsic line broadening. To overcome this difficulty, X-band measurements were performed resulting in a narrow powder pattern as shown in Fig. 6. If present, X-band observation should provide the best chance to resolve such hf splitting resulting from the H nucleus.[34] Yet, no such features are observed from where we conclude that for the fumed silica nanoparticles the observed g_c shift for the E' centers located in the surface layers does not concern a back bonded OH group. Thus, the previous interpretation is retained: For the nano-

particles the g_c shift most probably results from amorphous strain disorder affecting the defect's configuration.

B. SiO impact

To further analyze the influence of the presence of SiO during the SiO-vac. anneal we explicitly compared the current results with those obtained in a former study[8] for regular vacuum annealing at $T_{an} \sim 1005-1205$ °C. From Fig. 2 it can be seen that with the presence of SiO during the anneal, the E' density in the fume has increased. This increase becomes gradually more drastic at higher anneal temperatures. Within the interpretation of interaction of the fume network with released SiO molecules, yet without entering into atomic structural detail, this result might be understood on grounds of simple general stoichiometry: The incorporation of SiO in a $SiO_{2(x)}$ network will result in a net Si enrichment (or, equivalently, O deficiency). Thus, in the fumed silica nanoparticles, which have been evidenced to be O rich,[8] the incorporation of SiO might thus result in an increase of the number of oxygen vacancies, hence E' defect centers. For $T_{an} \sim 1205$ °C the total E' density becomes comparable to, even slightly higher than, the density obtained for bulk thermal SiO_2 ($\sim 1.4 \times 10^{17} g^{-1}$; standard quality).[35] It appears that the incorporation of SiO in the fumed silica network causes a serious degradation of the oxide quality in terms of oxygen vacancies. A similar increase in E' density has been observed before ascribed to the interaction of SiO with the SiO_2 network at elevated temperatures.[19,22] However, in those cases the ESR spectra obtained for $T_{an} \geqslant 1005$ °C were dominated by the S center suggested to be of the type $Si_nO_{3-n} \equiv Si\bullet$ ($n=1,2$).[19,36] No S center was observed in the current fumed silica sample indicating that the nanoparticle network structure is unfavorable for S center creation.

In addition to the difference in defect density, a noteworthy difference concerns the observed g_c value of the E' signal, as illustrated by Fig. 3. For the standard vacuum anneal the g_c value had shifted[8] to a somewhat higher value than the one typically observed in thermally grown SiO_2 on Si ($\Delta g_c \sim 0.0001$). This shift may be seen as originating from the presence of E' centers in the surface regions of the nanoparticles, with (somewhat) modified ESR parameters, i.e., enhanced g_c.[8] In the current case, where SiO-vac. anneal is applied, no such shift could be observed, indicating that there is no significant fraction of surface E' centers left after the SiO-vac. anneal, in which case more of the E' centers in the (near) surface region would have turned into bulk silica properties by the SiO impact. In another opinion this could indicate that while a larger fraction of surface E' centers would still be left, their contribution to the overall observed E' signal is insufficient to cause a significant shift in the observed g_c. This would mean that a fraction of ~40% is insufficient to experimentally induce a measurable g shift, as indeed confirmed by independent spectral simulations. This may find some support in the generally experimentally observed trend of a decreasing decay rate with increasing T_{an}. Anyhow, it can be stated that the E' centers generated during the SiO-vac. anneal exhibit predominantly core region properties. The surface regions and the core region appear to respond differently to penetrating SiO molecules.

C. Hyperfine interaction

1. Observed structure

In previous work, it has been pointed out that monitoring the properties (e.g., g_c value) of the central Zeeman ESR signal of embedded intrinsic E' centers as a function of post manufacture annealing and treatment (aging, VUV, and UV excitation) may provide useful information on the network structure of silica nanoparticles. As to the core region of these, no variation in the E' Zeeman signal, i.e., g_c shift, was observed compared to bulk a-SiO_2, from where it was concluded that the core is quite bulk-silica-like. Uchino *et al.*, however, obtained experimental infrared and Raman data[1] indicating that the structure of the core of the nanoparticles is not fully identical to that of bulk silica. If so, most probably then these alterations in the network are too small to engender a detectable g_c shift of embedded E' centers, leaving this "ESR route" unsuccessful. Here, the currently observed hf structure may come to the rescue (see Fig. 4). The signals are observed on fumed nanoparticle samples subjected to SiO-vac. annealing in room ambient for substantial time, the latter resulting in suppression of the presumed surface E' system. So, the observed E' hf structure (two doublets) would also pertain to the core part of the nanoparticles.

(a) Inner doublet. We can be short about the inner 73-G doublet, actually observed with splitting of 69 ± 4 G and 73 ± 2 G in the nanoparticles and suprasil reference, respectively. Extracting the hf parameters of this doublet from the fumed silica spectrum is strongly hampered through interference of the copresent OHC signal with the low-field doublet signal, as can be seen from Fig. 4, resulting in a reduced accuracy (± 4 G). To get more accurate information on the hf splitting spectral simulations were carried out using a code based on exact matrix diagonalization incorporating the Breit-Rabi formula.[37] For this end, it was assumed the high-power second harmonic spectra to resemble direct absorption shapes (χ''), an observation commented on previously,[26] for which empirical evidence has been provided. For suprasil the observed hf doublet could be well simulated, as shown in Fig. 5, using the isotropic parameters $g=2.0019$ and $A_{iso}=73$ G, where A_{iso} is the isotropic hf coupling constant; any anisotropic contributions remained unresolved. As to fumed silica, independent fitting of the hf doublet was even more severely obstructed by the overlapping OHC signal. However, if assuming that the g value of the hydrogen associated E' center is the same in suprasil and fumed silica (as it is for E'_γ), we may circumvent this hurdle. Using this in the fitting procedure and focusing on the high-field doublet signal, we obtained $A_{iso}=68$ G with an estimated accuracy of ± 2 G. In principle, similar to the primary 418-G doublet, the properties of this 73-G doublet could be perused as well to infer information about the properties of the core of the nanoparticles where the originating defects (O_2=Si˙-H) are built in (vide infra). Indeed, although on the limit of experimental accuracy, there may be a decrease in hf splitting compared to the reference sample. Yet the doublet seems less amenable

TABLE I. List of various theoretical estimates in the literature of the hyperfine coupling constants A_s and A_p for $3s$ and $3p$ electrons on atomic silicon. The O-Si-defect bond angle for the E'_γ defects in suprasil (θ_{bulk}) and fumed silica (θ_{nano}) are calculated from these values using Eq. (3). Assuming an accuracy of ±2 G on the measured isotropic hyperfine constant A_{iso}, the accuracy attained on θ is ±0.03°.

A_s (G)	A_p (G)	Ref.	θ_{nano}[b]	θ_{bulk}[b]	$\Delta\theta$[c]
1710	34	44 and 45	110.60°	110.32°	0.28°
1640[a]	41[a]	41	112.15°	111.86°	0.28°
1207[a]	31[a]	42	112.33°	112.04°	0.28°
1497[a]	38[a]	43	112.25°	111.97°	0.28°

[a]The cited hf coupling constants were reported in units of MHz. These are converted to units of G using $A(\text{G})=0.7144775\ g^{-1}\ A\ (\text{MHz})$, where $g=2.00055$, the zero-crossing g value of the E'_γ center.
[b]The absolute value of θ depends significantly on the theoretical values used in the calculation.
[c]The difference $\Delta\theta=\theta_{\text{nano}}-\theta_{\text{bulk}}$ in θ for the E' center in fumed silica and bulk silica gives the same value for the various theoretical estimates.

for that purpose for reasons such as attainable experimental accuracy (signal overlap) and the absence of a reference base linking hf structure parameters with SiO_2 network/material properties. Hence, we refrain from further hf analysis.

There is, however, one more interesting observation concerning the relative intensities of the H-doublet in fumed silica and suprasil. Observed many times before in various types of a-SiO_2, this 73-G doublet was assigned to the H-associated E'-type center O_2=Si˙-H, the hf splitting thus originating from the interaction of the unpaired electron with a proton in a back bond.[27,28] The defect thus signals the presence (though not exclusively, of course) of hydrogen in the silica network. In the second harmonic mode Q-band spectra (see Figs. 4 and 5), this doublet appears relatively more prominent for suprasil than for fumed silica. For equal spectroscopic behavior, this suggests that fumed silica nanoparticles contain less H. It should be added that this conclusion also assumes that the ESR-activation ratio of E'_γ/O_2=Si˙-H defects is effectuated equally by VUV and γ irradiation (applied to fumed silica and suprasil, respectively). Though perhaps plausible, this does not be a priori so, and some caution may be needed.

(b) Outer doublet. The observed second outer doublet concerns the primary ^{29}Si hf splitting of E' centers (the E'_γ variant)[16,29] located in the core of the nanoparticles. The hf parameters are analyzed to attain more in depth information on the core structure. From Fig. 4 it can clearly be seen that the primary ^{29}Si hf splitting of the E' center is larger in the fumed silica nanoparticles than for suprasil. To obtain more detailed information about the hf structure spectral simulations were carried out. For suprasil the observed hf doublet could be well simulated using similar ^{29}Si hf parameters ($A_\parallel$=462 G and $A_\perp$=396 G) as reported by Griscom *et al.* for glassy silica.[16] The g values used for this fitting procedure were taken from the simulation of the central line: g_1=2.0017, g_2=2.0005, and g_3=2.0002. The parallel ($A_\parallel$) and perpendicular ($A_\perp$) hf constants are linked to the isotropic (A_{iso}) part (s part: Fermi contact interaction) and the anisotropic (A_{aniso}) part (p part: dipolar interaction) of the hf interaction through the equations

$$A_\parallel = A_{\text{iso}} + 2A_{\text{aniso}}, \tag{1}$$

$$A_\perp = A_{\text{iso}} - A_{\text{aniso}}. \tag{2}$$

For the suprasil E'_γ center this results in A_{iso}=418 G and A_{aniso}=22 G.

As can be seen from Fig. 4, the copresent OHC signal is badly interfering with the low-field doublet signal, particularly so for the fumed nanoparticles, exhibiting a relatively stronger OHC component. This hampered independent fitting of the primary ^{29}Si hf doublet for fumed silica. Therefore, based on various hf constants reported in the literature,[16,17] and in a similar attitude as taken before we assumed that the increase in the measured hf splitting for the E' center in fumed silica is mainly caused by an increase in the isotropic part of the hf interaction. Thus, in the fitting procedure A_{aniso}(=22 G) was kept constant, which enables a clear comparison with data from the literature. For the primary ^{29}Si hf parameters of the E' center in the fumed silica nanoparticles, this led to the results $A_\parallel$=480 G and $A_\perp$=414 G or, put differently, A_{iso}=436 G and A_{aniso}=22 G. The inferred A_{iso}, A_{aniso} values provide access to the structure of the corresponding E' centers.

2. E' defect structure

Within the assumptions of perfect sp^3 hybridization and specific bond-direction-orbital relationships, the hf interaction is related to the O-Si-defect bond angle θ according to (see, e.g., Refs. 16, 38, and 39)

$$\tan\theta = -\left[2\left(1+\frac{A_{\text{aniso}}}{A_p}\frac{A_s}{A_{\text{iso}}}\right)\right]^{1/2}, \tag{3}$$

where A_s and A_p are the hf coupling constants for $3s$ and $3p$ electrons on atomic silicon. Using this equation and the inferred A_{iso}, A_{aniso} values,[40] we have for various theoretical values of A_s and A_p existing in the literature[41–45] calculated the bond angle θ for E' in fumed silica (θ_{nano}) and suprasil (θ_{bulk}). The results are listed in Table I, showing that the inferred absolute value for θ depends on the used set of theoretical estimates for A_s and A_p leaving some dissatisfaction. Fortunately, as to the difference $\Delta\theta \equiv \theta_{\text{nano}} - \theta_{\text{bulk}}$ in bond angle between fumed silica and suprasil the existing spread among various theoretical estimates has less impact,

all estimates leading to about the same $\Delta\theta$ of $\sim 0.3°$. But, clearly, when comparing absolute values of θ reported in the literature, one should cautiously ensure that the same theoretical values for A_s, A_p have been used. Using the values for A_s and A_p cited by Morton and Preston,[41] still regarded as most accurate, we obtain $\theta_{\text{bulk}}=111.86°$ and $\theta_{\text{nano}}=112.15°$, so $\Delta\theta=0.28°$. The inferred value for θ is somewhat larger for the E'_γ center in the core of the nanoparticles pointing to a configurationally more (sharpened) pyramidal E' defect.[46]

It should also be noted that besides the theoretical values used for A_s and A_p an even bigger influence on the inferred value for θ comes from the bond angle-hf interaction relationship used [e.g., Eq. (3)] and, by extend, the assumptions made in its derivation. Various (first principles) theoretical analyses were made. Edwards and Fowler[39] suggested the use of the wave functions from $Si^{(+1)}$ instead of the neutral atomic wave functions, as a way to include the ionicity of the sp^3 hybridisation in SiO_2. Applying their corrected wave functions to Eq. (3) would result in our case, in (slightly) higher values for θ ($\theta_{\text{bulk}}=113.4°$ and $\theta_{\text{nano}}=113.7°$ for the E' center in suprasil and fumed silica, respectively) but still similar values for $\Delta\theta$ are obtained. More alarmingly however, based on self-consistent field (SCF) LCAO calculations, these authors concluded that Eq. (3), though qualitatively consistent, is blatantly inadequate: A much weaker dependence (~ 6 times) of A_{iso} on θ (larger variation in θ with A_{iso}) is found and conclude there is no simple relationship between bond angles and hf parameters for Si DB-type defects. The SCF result would give $\theta_{\text{nano}}=117.2°$ vs $\theta_{\text{bulk}}=113.2°$ ($\Delta\theta=4°$), a much stronger increase in θ for the fumed silica. This much enhanced variation of θ with A_{iso} was confirmed later by Pacchioni and Vitiello[47] from first-principle Hartree-Fock and density-functional-theory calculations. For the range of θ values from 100 to 118°, they obtained an increase in A_{iso} of ~ 3.5 G for an increase in θ of 1° (giving $\Delta\theta\sim 5.8°$). It appears that the A_{iso}-θ relationship as laid down in Eq. (3) is quantitatively inexact.[48] However, qualitatively, the trends in the physical picture are retained: A_{iso} increases along with θ. Thus (further) usage of Eq. (3) appears only "justified" as a handy means (analytic expression) to point out the physical trends qualitatively: According to in-depth theory, variations in θ with A_{iso} are underestimated by an order of magnitude.[49] On this notion it may still be appropriate to continue using the results obtained from Eq. (3).

Having attained a specific quantification for a change in the structure of the E' center between bulk silica and the core of silica nanoparticles, we may want to transfer this information to assessing how it would affect other experimental quantities, such as, the g value of the ESR resonance. As already mentioned, generally, such a structural modification does not only affect the hf splitting but will also result in a g shift. However, for the core E' centers no shift could be detected, which then must mean that the variations in θ remain most probably too small to result in a detectable g shift. For the surface E' system a g shift (increase) was observed, indicating that the variations for θ are stronger for the outer layers of the nanoparticles. But here, whether the surface E' centers have a more planar or pyramidal defect structure remains unknown as no hf structure could be resolved due to sensitivity reasons. So, unfortunately, no direct experimental link can be provided between shift in g and change in structural pyramidality. The answer may be provided by theory. However, if assuming that the E' centers in the surface layers follow the same trend, but more pronounced, as their counterparts located in the core regions, i.e., enhanced pyramidality, than we would reach the conclusion that an increase in θ is accompanied by an increase in g. This result would be consistent with theoretical work reported for the unpaired Si bonds in a-Si and the P_b center,[50] where an increase in g_c value is linked with an increase in θ and hence a more pyramidal defect structure.

3. Densification

While the attained atomic scale information on the structure of a specific point defect would be of interest on its own right, the next step beyond in analysis reaches a main goal. Very basically, it touches the potentiality of (intrinsic) point defects in providing pertinent information on larger scale structural/material physical quantities of the solid matrix these are embedded in—what can an atomic scale point defect tell us about its broader environment? The potentiality of point defects in this sense is underlied by many examples before, e.g., P_b defects at Si/SiO_2 interfaces,[11,51] Fe impurities in Si.[52] Assessing this is a main goal. As to the current nanoparticles, the increase observed in A_{iso} for the E' centers residing in the core of the nanoparticles as compared to bulk silica may also provide in depth information on more global structural/material parameters of the matrix the defects are embedded in. As starting point we have compiled in Table II the results of the primary ^{29}Si hf splitting of the E' center for the current nanoparticles and for glassy SiO_2 reported in the literature.[10,16–18,26,27,53,54] Over the various values, excluding densified and ^{29}Si implanted samples, an average hf splitting A_{iso} of 419 ± 4 G is attained. A substantial increase in splitting is seen to result from densification, as well as, though somewhat less, from Si implantation. As the latter was outlined also to effectuate densification,[53,54] there appears a clear link between densification and enhancement of ^{29}Si hf splitting. Thus, such an increase in A_{iso} has been observed before[17,18,53,54] and is assigned to a densification of the a-SiO_2 matrix. In a remarkable ESR study of the hf splitting of the E' center in a-SiO_2 as a function of the density[17] for samples densified under hydrostatic pressure at high temperatures, Devine and Arndt reported an increase in A_{iso} with growing silica density. These results did not depend on the type of silica, so it seems reasonable that their inferences can also be applied for the analysis of the current fumed silica data. In this view the obtained fractional increase in A_{iso} of 4.1% would imply a densification of the fumed silica network of 5.9%, corresponding to an increase in specific gravity to 2.33 g cm^{-3} as compared to 2.202 g cm^{-3} for undensified silica. The core of the nanoparticles is thus found to be densified.

But how does this densification come about in terms of modification of the SiO_2 network? In addition to ESR, Devine *et al.* also performed x-ray scattering, Raman, and NMR measurements on densified silica.[55] From these results they concluded that the densification produces a decrease in the

TABLE II. Comparison of experimental data on the primary ^{29}Si hyperfine splitting (A_{iso}) of E'_γ centers in various bulk silica glasses.

hf splitting (G)	Ref.	Sample	Damaging agent
423	16	Corning 7940	~100 Mrad(Si) ^{60}Co γ rays
423	16	Corning 7943	~100 Mrad(Si) ^{60}Co γ rays
423	16 and 26	Suprasil 1	~100 Mrad(Si) ^{60}Co γ rays
423	16	Suprasil N-1	~100 Mrad(Si) ^{60}Co γ rays
423	16	Dynasil 1000	~100 Mrad(Si) ^{60}Co γ rays
423	16	NRL high purity precipitated silica	~100 Mrad(Si) ^{60}Co γ rays
418	16	95% ^{29}Si enriched SiO_2	~100 Mrad(Si) ^{60}Co γ rays
420	26	95.3% ^{29}Si enriched SiO_2	~100 Mrad(Si) ^{60}Co γ rays
420	26	99.8% ^{29}Si enriched SiO_2	~100 Mrad(Si) ^{60}Co γ rays
418	27	High OH silica spectrosil rods (~1200 ppm OH)	~100 Mrad(Si) ^{60}Co γ rays
418	27	Suprasil 2 powder; high OH +OD	~100 Mrad(Si) ^{60}Co γ rays
410	17	Suprasil I	76 Mrad(Si) ^{60}Co γ rays
410	17	Suprasil W1	76 Mrad(Si) ^{60}Co γ rays
465	17	Suprasil I; ~24% densified	76 Mrad(Si) ^{60}Co γ rays
465	17	Suprasil W1; ~24% densified	76 Mrad(Si) ^{60}Co γ rays
465	18	Suprasil 1 (OH > 1200 ppm); 24.1% densified	248-nm KrF laser irradiation
440	53	Wet synthetic SiO_2 glass (type II, OH conc. $\sim 3\times 10^{19}$ cm^{-3}); ^{29}Si implanted	^{29}Si implantation
420	10	Fused silica glass powder	8.3×10^2 Mrad(Si) ^{60}Co γ rays
420	10	Suprasil 1	8.3×10^2 Mrad(Si) ^{60}Co γ rays
440	54	Dry a-SiO_2 (type II, OH conc. $\leqslant 10^{17}$ cm^{-3}); ^{29}Si implanted	^{29}Si implantation
418 ± 2 G	This work	Suprasil I synthetic silica[a]	100 Mrad(Si) ^{60}Co γ rays
438 ± 2 G	This work	Fumed 7 nm particles; 1105 °C SiO-vac. anneal	10 eV photons[b]

[a]See Ref. 25.

[b]Obtained from a Kr-resonant discharge lamp; flux ~10^{15} cm^{-2} s^{-1}.

oxygen-second-nearest-neighbor-oxygen separation (R). So, R is the minimum distance of the closest approach of two oxygen atoms belonging to adjacent SiO_4 tetrahedra. As a next invoked link, one calculation concludes that restrictions on interoxygen distances impose limits on possibly occurring ring configurations of SiO_4 tetrahedra in the SiO_2 network (steric hindrance model).[56] In combination, the observed densification-induced reduction in average R led to the suggestion that the observed remnant "plastic" densification (~15% after returning the sample to standard pressure) involves modification of the intrinsic ring structure of a-SiO_2, now perhaps being permitted by the formation of low membered rings previously excluded through distance constraints. The description of the disordered silica network in terms of the distribution of occurring n-membered rings ($n=3-7$) is a well known approach (see, e.g., Ref. 57 for a comprehensible overview), and there is a general consensus the structure to contain ring structures of different sizes,[57] including planar three-membered and puckered four-membered rings, as concluded from Raman spectroscopy.[58] The average ring size in standard bulk vitreous SiO_2 is ~6.[57] The calculations infer that a decrease in R is indicative for the presence of relatively more low membered rings. At least the existence of such configurations is no longer excluded through distance considerations. On the basis of the previous inferences, our E' hf ESR data would indicate an enhanced fraction of lower membered (SiO_4 tetrahedra) rings in the core part of silica nanoparticles compared to bulk silica.[46]

Generally, we can conclude that our ESR results in combination with previous results linking increase in ^{29}Si hf splitting of E' centers with densification, point to densification of the interior of fumed silica nanoparticles compared to undensified bulk silica, tentatively linked to a modification of the distribution in occurring ring structures in the fumed

silica network. These results confirm independently those of Uchino *et al.*[1] reporting that the core of the nanoparticles differs from bulk silica in that it would be comprised of more low ($n=3$ and 4) membered rings.

4. Densification and ring structure

For scientific objectivity, it is important to add a remark regarding the apparently above attained inference that enhanced density would correlate with the presence of an enhanced fraction of low ($n=3,4$) membered rings at the cost of larger rings. Such inference seems not the mainstream one emerging from the general topology considerations of bulk disordered silica in terms of (network) statistics of rings of SiO_4 tetrahedra.[57] So, some caution not to jump recklessly to oversimplified conclusions seems at place. On grounds of a comparison of n-fold primitive ring content of tetrahedral c-silica polymorphs stable at low temperatures,[57] it appears that the average ring size rather increases with density, which seemingly paradoxical observation is understood in the sense that larger rings may fold back on themselves in a way that more constrained smaller rings cannot. At the same time, there appears no regular correlation of density or topology with the intertetrahedral Si-O-Si mean bridging bond angle, although for fixed angle topology, lowering of this angle (with correlated increase in θ) would result in a density increase. So, the current inference for fume silica particles about a link between increased density and enhanced fraction of low membered rings might not be sustained by topological insight for bulk silica.

However, it is important to recognize that the above mentioned topological insight pertains to bulk properties of disordered silica. This may not just straightforwardly apply to the current fume particles, for which in fact, there exist ample experimental[1–3] and theoretical[59,60] evidence. In support, if assuming for a 7-nm-sized silica particle, which contains ~4000 SiO_4 tetrahedra, a surface layer of about 0.35-nm thick (~1 SiO_2 layer), about 27% of the particle is surface, increasing to ~48% if taking a ~0.7-nm-thick surface layer. So, it is not unreasonable to expect a large impact of the surface area, i.e., the particle's network nature may be entirely dominated by constraints resulting from energy-minimization driven surface reconstruction, drastically affecting the interior. Our current findings may then rather comply with the topological point of view based on the metric where the parts belonging to the topological surface are defined as including every tetrahedron whose local cluster (i.e., the set of all tetrahedra belonging to the rings passing through a given tetrahedron) contains a surface tetrahedron.[57] Interestingly, energy-driven surface reconstruction has been observed to result in the formation of low ($n=3$) member rings as a natural fact.[61] So, in this picture, there appears no conflict between conventional topological insight of bulk silica and current results on nanosilica particles.

As a corollary of this discussion on prevailing ring size, there may appear a conflict with insight in defect formation. From their work, Uchino *et al.*[1] conclude that fume silica particles contain both more three and four membered rings than bulk silica (as supported here by ESR data in the indirect sense of the occurrence of densification, possibly linked to an enhanced fraction of lower n rings). In separate work,[62,63] it was concluded that the highly strained three-membered rings are the precursors for E' and OHC centers. Yet, in the VUV-irradiated fume particles, we find the E' density to be far lower (~100 times) than typical for thin (~4.1–6.5 nm) thermally grown a-SiO_2 on Si,[8] meeting high-quality bulk silica properties. So, if the previous conclusion on the enhanced presence of $n=3$ rings were correct, it would imply that these rings cannot be the precursors of E' centers, at least not in the direct sense. This remains currently elusive.

V. SUMMARY

An ESR study has been carried out on fumed silica nanoparticles subjected to post manufacture heating in the presence of an (100)Si/SiO_2 interface and additional VUV irradiation. With a view to improve structural insight, the atomic properties of the $SiO_{2(x)}$ network of the nanoparticles have been assessed using intrinsic defects, i.e., E' centers (O vacancies), as local atomic probes. The results demonstrate that the hf parameters are more sensitive to changes in the network structure than the g matrix, or in the central Zeeman signal in general.

The presumed interaction of volatile SiO at high temperatures in vacuum with the $SiO_{2(x)}$ network leads to an increase in the density of E'_γ centers, observed after VUV activation. This indicates that the fumed silica network is vulnerable for SiO attack, possibly effectuating Si enrichment leading to an increase in O vacancy (E'_γ) density. This would bring the fumed silica network closer to the compositional properties of bulk SiO_2 with known superior quality. Yet, the SiO influence does not appear to be uniform throughout the nanoparticle, as the surface regions and the core region respond differently to interaction with SiO molecules.

The high-T SiO-treatment-induced drastic increase in E'_γ defect density has enabled the detection of the primary ^{29}Si E'_γ hf structure. Consistent fitting revealed a larger isotropic hf constant for the fumed silica nanoparticles than for suprasil (bulk unstrained silica), leading to at least two principle pieces of information: First, as the hf parameters are linked with the O-Si-defect bond angle θ this result, interpreted within basic theory, indicates that θ is larger for fumed silica than bulk SiO_2, that is, a more sharpened pyramidal structure of E'_γ centers in fumed silica. Second, on the basis of previous work, the observed increase in A_{iso} points to densification of the SiO_2 core of the nanoparticles. According to previous interpretation this is possibly due to a modification of the distribution of occurring ring structures in the fumed silica network suggesting the presence of more low-membered rings of SiO_4 tetrahedra. However, the less obvious nature of the latter inference within the basic topological insight for bulk disordered silica requires caution. It may concern exclusive properties of the nanosize, and will be interesting to pursue further.

In addition to the primary ^{29}Si E' hf doublet a H-associated doublet assigned to $O_2{\equiv}\dot{S}i$-H entities was additionally observed. Relatively to the ordinary E' signal, this doublet is found to be less prominent in the spectra of fumed

silica than suprasil indicating that the nanoparticles would contain less hydrogen.

As a general conclusion, the obtained results illustrate that detailed ESR studies of the specific ESR parameters such as the g and hf matrix of an embedded probing inherent point defect (such as E') can provide valuable information on the specific network structure on atomic scale—in the current case, of nanosized particles.

ACKNOWLEDGMENTS

One of the authors (A.S.) is grateful to L. W. Hobbs for fruitful discussions regarding ring structures in silica.

[1] T. Uchino, A. Aboshi, S. Kohara, Y. Ohishi, M. Sakashita, and K. Aoki, Phys. Rev. B **69**, 155409 (2004).
[2] I. S. Altman, D. Lee, J. D. Chung, J. Song, and M. Choi, Phys. Rev. B **63**, 161402(R) (2001).
[3] T. Uchino, A. Sakoh, M. Azuma, M. Takano, M. Takahashi, and T. Yoko, J. Phys.: Condens. Matter **14**, 11111 (2002).
[4] H. Saito and T. Hyodo, Mater. Sci. Forum **255-257**, 463 (1997).
[5] B. C. Bunker, D. M. Haaland, T. A. Michalske, and W. L. Smith, Surf. Sci. **222**, 95 (1989).
[6] C. C. Liu and G. E. Maciel, J. Am. Chem. Soc. **118**, 5103 (1996).
[7] S. M. Prokes, W. E. Carlos, L. Seals, S. Lewis, and J. L. Gole, Mater. Lett. **54**, 85 (2002).
[8] A. Stesmans, K. Clémer, and V. V. Afanas'ev, Phys. Rev. B **72**, 155335 (2005).
[9] A. Stesmans, K. Clémer, and V. V. Afanas'ev, J. Phys.: Condens. Matter **17**, L393 (2005).
[10] D. L. Griscom and M. Cook, J. Non-Cryst. Solids **182**, 119 (1995).
[11] A. Stesmans, Phys. Rev. B **48**, 2418 (1993).
[12] F. Gerson and W. Huber, *Electron Spin Resonance Spectroscopy of Organic Radicals* (Wiley, Darmstadt, 2003).
[13] D. L. Griscom, Nucl. Instrum. Methods Phys. Res. B **46**, 12 (1990).
[14] W. L. Warren, E. H. Poindexter, M. Offenberg, and W. Müller-Warmuth, J. Electrochem. Soc. **139**, 872 (1992).
[15] P. G. Tello, V. V. Afanas'ev, and A. Stesmans, Microelectron. Eng. **72**, 81 (2004); A. Stesmans and V. V. Afanas'ev, J. Appl. Phys. **97**, 033510 (2005).
[16] D. L. Griscom, E. J. Friebele, and G. H. Sigel Jr., Solid State Commun. **15**, 479 (1974).
[17] R. A. B. Devine and J. Arndt, Phys. Rev. B **35**, 9376 (1987).
[18] R. A. B. Devine and J. Arndt, Phys. Rev. B **42**, 2617 (1990).
[19] A. Stesmans, B. Nouwen, and V. V. Afanas'ev, Phys. Rev. B **66**, 045307 (2002).
[20] R. Tromp, G. W. Rubloff, P. Balk, F. K. Le Goues, and E. J. van Loenen, Phys. Rev. Lett. **55**, 2332 (1985).
[21] A. Stesmans and V. V. Afanas'ev, Appl. Phys. Lett. **69**, 2056 (1996).
[22] A. Stesmans and V. V. Afanas'ev, Microelectron. Eng. **36**, 201 (1997).
[23] Y. Takakuwa, M. Nihei, and M. Miyamoto, Jpn. J. Appl. Phys., Part 1 **32**, L480 (1993); **177/118**, 141 (1997).
[24] Sigma-Aldrich Inc., Missouri, USA.
[25] Obtained from Heraeus (Germany) containing [OH] $\sim$1200 ppm (by weight); $[H_2O] \leqslant 600$ ppm, and total metal content <1 ppm.
[26] D. L. Griscom, Phys. Rev. B **20**, 1823 (1979).
[27] T. E. Tsai and D. L. Griscom, J. Non-Cryst. Solids **91**, 170 (1987).
[28] J. Vitko, Jr., J. Appl. Phys. **49**, 5530 (1978).
[29] R. H. Silsbee, J. Appl. Phys. **32**, 1459 (1961).
[30] V. A. Radzig, in *Defects in* SiO_2 *and Related Dielectrics: Science and Technology, NATO Science Series, Series II: Mathematical and Physical Chemistry*, edited by G. Paccioni, L. Skuja, and D. L. Griscom (Kluwer Academic Publishers, Dordrecht, 2000), p. 339.
[31] V. A. Radzig, Colloids Surf., A **74**, 91 (1993).
[32] W. L. Warren, E. H. Poindexter, M. Offenberg, and W. Müller-Warmuth, J. Electrochem. Soc. **139**, 872 (1992).
[33] G. Hochstrasser and J. F. Antonini, Surf. Sci. **32**, 644 (1972).
[34] A. A. Bobyshev and V. A. Radzig, React. Kinet. Catal. Lett. **29**, 551 (1988).
[35] P. G. Tello, V. V. Afanas'ev, and A. Stesmans, Microelectron. Eng. **72**, 81 (2004); A. Stesmans and V. V. Afanas'ev, J. Appl. Phys. **97**, 033510 (2005).
[36] A. Stirling and A. Pasquarello, Phys. Rev. B **66**, 245201 (2002).
[37] G. Breit and I. I. Rabi, Phys. Rev. **38**, 2082 (1931).
[38] A. R. Reinberg, J. Chem. Phys. **41**, 850 (1964).
[39] A. H. Edwards and W. B. Fowler, Phys. Rev. B **41**, 10816 (1990).
[40] As stated, A_{aniso} has been fixed at 22 G in the current analysis. Instead, in another approach one may (see, e.g., Ref. 17), starting from measured A_{iso} data, keep constant over the altering defect configuration (pyramidality) the $3s$ plus $3p$ electron spin density of the defect orbital $\psi = c_s|3s\rangle + c_p|3p\rangle + \Sigma_i c_i|\mathrm{other}\rangle$, e.g., at $c_s^2 + c_p^2 = 0.8$. In our case, this would result in $\Delta\theta = 0.48°$. While enlarged, the trend remains, but bears out how critically inferences about θ depend on wave function subtleties.
[41] J. R. Morton and K. R. Preston, J. Magn. Reson. (1969-1992) **30**, 577 (1978).
[42] A. K. Koh and D. J. Miller, At. Data Nucl. Data Tables **33**, 235 (1985).
[43] C. G. Van de Walle and P. E. Blöchl, Phys. Rev. B **47**, 4244 (1993).
[44] W. Kohn and J. M. Luttinger, Phys. Rev. **97**, 883 (1955).
[45] R. G. Barnes and W. V. Smith, Phys. Rev. **93**, 95 (1954).
[46] As to this conclusion, one may conjecture that observation of the ^{29}Si E' hf structure has been enabled through interaction with SiO at high T (E' density enhancement), which may have resulted in significant modification of the SiO_2 network so that the current results would not pertain to the pristine nanoparticle properties. The impact, however, on the global network structure is considered minor given the still low maximum density of E' defects ($\sim 1 \times 10^{17}$ cm^{-3}) in the SiO_2 matrix ($\sim$5 at. ppm) of the fume samples for which the hf data are currently reported ($T_{\mathrm{an}} \sim 1105$ °C).

[47] G. Pacchioni and M. Vitiello, Phys. Rev. B **58**, 7745 (1998).
[48] On this account there may appear some internal consistency conflict in the literature, at least as far as densified silica is concerned. Using Eq. (3), which appears inadequate, Devine *et al.*, found from ESR hf data of E'_γ centers a decrease in mean neighboring Si-O-Si bridging bond angle of $\sim 5.1°$ in densified silica (16–24 %), in excellent agreement with that inferred from x-ray scattering and NMR studies (Refs. 17 and 55).
[49] Edwards and Fowler (Ref. 39) concluded that Eq. (3) is not useful for determining either the absolute value or occurring range of the Si-O-DB angle θ from observed hf data for threefold coordinated paramagnetic point defects, such as E'_γ, pointing out that assumptions underlying its derivation are invalid. From various theoretical calculations (Refs. 39 and 47) there appears no simple analytic relationship between unpaired bond angles and hf parameters. The relationship is influenced by energetic as well as geometric effects, and one has to resort to computational evaluation.
[50] N. Ishii, M. Kumeda, and T. Shimizu, Jpn. J. Appl. Phys. **20**, L673 (1981); Y. Fu and P. A. Fedders, Solid State Commun. **84**, 799 (1992).
[51] K. L. Brower, Phys. Rev. B **33**, 4471 (1986); J. T. Yount, P. M. Lenahan, and P. W. Wyatt, J. Appl. Phys. **77**, 699 (1995).
[52] W. Gehloff and K. H. Segsa, Phys. Status Solidi B **115**, 443 (1983).
[53] H. Hosono, H. Kawazoe, K. Oyoshi, and S. Tanaka, J. Non-Cryst. Solids **179**, 39 (1994).
[54] M. Mizuguchi, H. Hosono, and H. Kawazoe, Mater. Sci. Eng., B **53**, 38 (1998).
[55] R. A. B. Devine, R. Dupree, I. Farnan, and J. J. Capponi, Phys. Rev. B **35**, 2560 (1987).
[56] Y. T. Thatachari and W. A. Tiller, J. Appl. Phys. **57**, 1805 (1985).
[57] L. W. Hobbs and X. Yuan, in *Defects in* SiO_2 *and Related Dielectrics: Science and Technology, NATO Science Series, Series II: Mathematical and Physical Chemistry* edited by G. Paccioni, L. Skuja, and D. L. Griscom (Kluwer Academic Publishers, Dordrecht, 2000), p. 37.
[58] K. Awazu and H. Kawazoe, J. Appl. Phys. **94**, 6243 (2003).
[59] I. V. Schweigert, K. E. J. Lehtinen, M. J. Carrier, and M. R. Zachariah, Phys. Rev. B **65**, 235410 (2002).
[60] A. Roder, W. Kob, and K. Binder, J. Chem. Phys. **114**, 7602 (2001).
[61] F. L. Galeener, J. Non-Cryst. Solids **49**, 53 (1982).
[62] H. Hosono, Y. Ikuta, T. Kinoshita, K. Kajihara, and M. Hirano, Phys. Rev. Lett. **87**, 175501 (2001).
[63] D. Donadio and M. Bernasconi, Phys. Rev. B **71**, 073307 (2005).